UCLA
UCLA Previously Published Works

Title

Study and analysis of contiguous channel triplexer based on combining method of two filtering circuits using CRLH and RH isolation circuits

Permalink

https://escholarship.org/uc/item/71d7f0jk

Journal

International Journal of Microwave and Wireless Technologies, 6(3-4)

ISSN

1759-0787

Authors

Lee, Hanseung
Wu, Chung-Tse Michael
Itoh, Tatsuo

Publication Date

2014-06-01

DOI

10.1017/s1759078714000178

Peer reviewed

Study and Analysis of Contiguous Channel Triplexer Based on Combining Method of Two Filtering Circuits Using CRLH and RH Isolation Circuits

Hanseung Lee, Chung-Tse Michael Wu, and Tatsuo Itoh

University of California at Los Angeles, 420 Westwood Plaza, Los Angeles, California, USA.

Several types of multiplexers based on isolation circuits have been introduced and investigated. Combining method of two filtering circuits (CMTC) is one way to make multiplexers based on isolation circuits. This method fits well for designing contiguous channel triplexers. A triplexer based on CMTC consists of a conventional transmission line (TL) connected to a diplexer and a composite right/left handed (CRLH) TL connected to a filter. The triplexer based on CMTC has two significant advantages. One is that it is not necessary to modify the design of a stand-alone filter and diplexer and there is freedom in the choice of filtering circuits. In addition, a designer does not need to perform 3-D full-wave optimization, because of a simple and straightforward design concept. In this paper, a triplexer prototype having 1 GHz, 1.125 GHz, and 1.25 GHz center frequencies, is designed and fabricated. The measured results show good agreement with the simulation results.
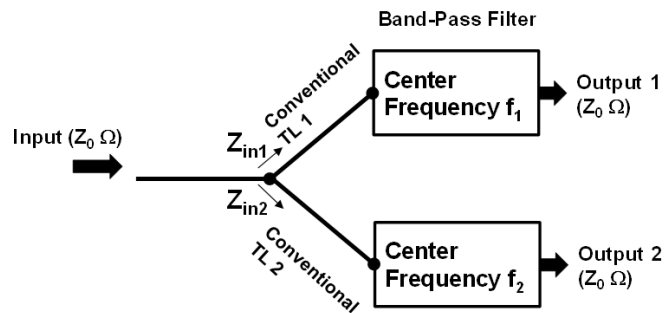
Corresponding author: Hanseung Lee; email: hlee0411@ucla.edu; phone: +1 310 733 6495

INTRODUCTION

In modern communication systems, it is necessary to be able to handle multiple frequency bands. If two or three communication standards can be processed through one base station for a mobile phone, its construction price will be lowered with concomitant benefits for customers. Multiband is already common to cell phone designs for handling GPS, WiFi, and cellular bands. In order to support such multiband systems, a multiplexer is necessary if only one antenna covers all the designated spectra. Many researchers have investigated design methods for multiplexers which can be categorized by star junction type and manifold junction type [1]-[9]. In both star junction and manifold junction type multiplexers, modification of filters and a complex optimization process are usually required. However, the

capability of using commercial filters without any modification in a simple design method would be attractive for a system designer. Fig. 1 (a) shows a diplexer made of two isolation circuits satisfying such demand. Each isolation circuit consists of a conventional right-handed (RH) transmission line (TL) connected to a filter, and it has open-circuit input impedance at the center frequency of the other channel. Hence the signal passes through one path while it is rejected by the other. Fig. 1 (b) shows the star-junction triplexer based on dual-band isolation circuits [10]. Similarly to the diplexer shown in Fig. 1 (a), each isolation circuit isolates itself from the input port at two operating frequencies of other circuits. In this concept, a composite right/left handed (CRLH) TL having dual-band characteristic is essential [11][12], because the isolation circuits used for the triplexer should be designed to have the isolation characteristic at two frequencies. However, this method is more difficult for a contiguous or narrow guard band triplexer than the concept of a triplexer based on combining method of two filtering circuits (CMTC) shown in Fig. 1 (c). The reason for this comes from the intrinsic characteristic of a band-pass filter (BPF) and a phase response of a CRLH TL. In the following section, detailed investigation will be discussed.
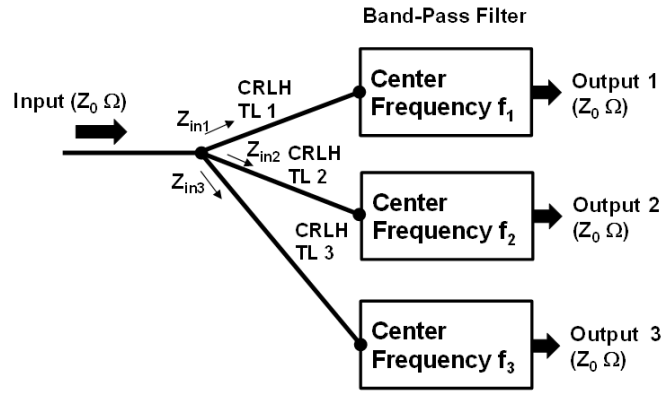
In this paper, the contiguous channel triplexer based on CMTC is presented. The concept of the triplexer and the theory for an isolation circuit are explained. Also, the reason why the proposed method is attractive for a contiguous channel triplexer is investigated. The design process and the measured results of the proposed triplexer are also provided.

(a)
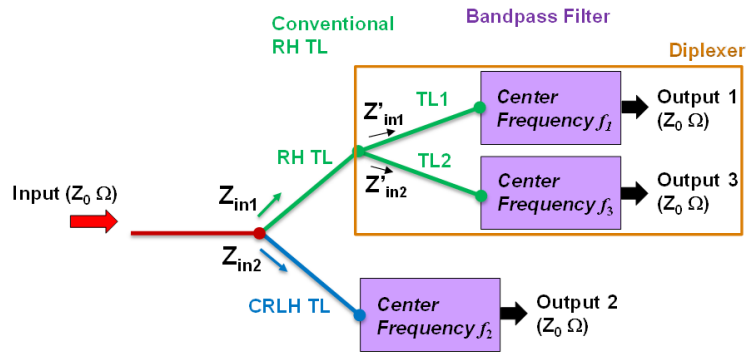
Fig. 1. Diagrams and operation concepts of multiplexers. (a) Diplexer based on isolation circuits. (b) Star-junction triplexer based on isolation circuits. (c) Proposed triplexer based on CMTC.

THEORY

A)   Combining Method of Two Filtering Circuits

The general combining method of two filtering circuits (CMTC) represented in Fig.2 uses two isolation circuits, as in the diplexer of Fig. 1(a) [13][14]. The difference between the diplexer and the CMTC is the use of a multi-band TL and a multiplexer, instead of a conventional RH

TL and a filter. Since the CMTC uses a multi-band TL to combine multiplexers instead of an individual filter, it requires fewer isolation circuits compared to the star-junction multiplexer based on isolation circuits. The operation concept is also represented in Fig. 2. The isolation circuit, comprising an N_2-band TL and an N_1-channel multiplexer, has open-circuit impedance at the operating frequencies of the other isolation circuit (from f_{N1+1} to f_{N1+N2}). On the other hand, the second isolation circuit, consisting of an N_1-band TL and an N_2-channel multiplexer, is isolated from the input port at frequencies from f_1 to f_{N1}. Therefore, one circuit allows a signal path while the other circuit prevents a signal flow. For example, a signal having an f_1 frequency cannot enter the second isolation circuit, but the signal goes through the N_2-band TL of the first isolation circuit. Thereafter the signal is only detected at output port 1 because of the frequency selective characteristic of the N_1-channel multiplexer. The frequencies from f_1 to f_{N1+N2} do not need to be in ascending order as shown in Fig. 2.

The proposed triplexer ($N_1 = 2$ and $N_2 = 1$) is based on CMTC, and the diagram is shown in Fig. 1(c). The triplexer comprises two isolation circuits. One is composed with a CRLH TL and a filter. Another isolation circuit comprises a conventional TL connected with a diplexer. In this paper, the diplexer is also made by the use of CMTC presented in Fig. 1(a) with $N_1 = 1$ and $N_2 = 1$. In Fig. 1(c), the frequencies, in ascending order, are f_1, f_2, and f_3, and the center frequency of the filter used on CRLH isolation circuit should be f_2 for easier design of the CRLH TL, and this will be explained in the section II-C.
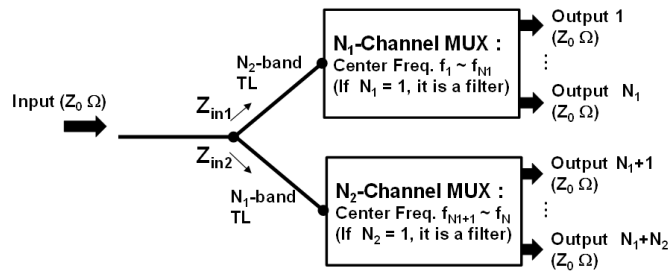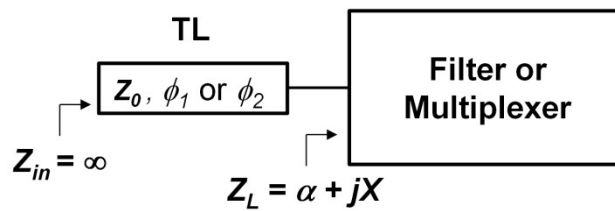

Fig. 2. Diagram and operation concept of combining method of two filtering circuits, where N_1 and N_2 are integer and $N = N_1 + N_2$.
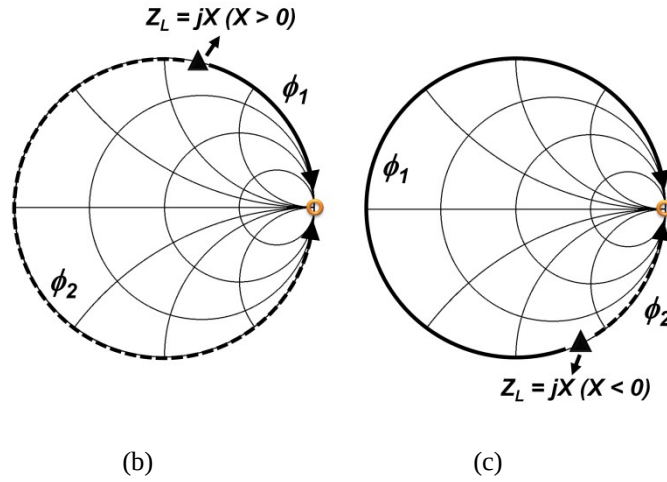

(a)

Fig. 3. (a) An isolation circuit diagram. (b) An example of the input impedance Z_L shown on the Smith chart (case 1: X > 0 and α = 0). (c) An example of the input impedance Z_L shown on the Smith chart (Case 2: X < 0 and α = 0).

B)   Isolation Circuit

Fig. 3(a) shows the diagram of an isolation circuit. The main function of this is having infinite input impedance at the target frequency. If it is far from the target frequency, the isolation circuit will lose its isolation characteristic. In the isolation circuit design, it is essential to determine a proper phase response of a TL and to design the TL with solved phase response. Each triangle in Fig. 3(b) and (c) shows an input impedance of a filter or a multiplexer at target frequency. In both cases, the real part of the impedance (α) is assumed zero for simplicity. A positive imaginary impedance and a negative imaginary impedance are shown in Fig. 3(b) and (c), respectively. In order to have open-circuit impedance, a phase change is necessary for which a TL can be used. A clockwise rotation shows a right-handed (RH) phase response, ϕ_1, having a negative value. A LH phase response, ϕ_2, has a positive value and it is represented as a counter-clockwise rotation in the Smith chart. ~~A conventional RH TL cannot provide a LH phase response, however such response can be realized by means of a CRLH TL.~~ To solve phase responses ϕ_1 and ϕ_2, one can use the transmission line impedance equation [15],

$$Z_{in} = Z_0 \frac{Z_L + jZ_0\tan(-\phi_{1,2})}{Z_0 + jZ_L\tan(-\phi_{1,2})} . \quad (1)$$

Since the input impedance of the circuit Z_{in} should be infinite, the denominator of (1) is zero, and the required phase response, $\phi_{1,2}$, is

$$\phi_1 = \begin{cases} -\arctan(Z_0/X), & X > 0 \\ -\pi - \arctan(Z_0/X), & X < 0 \end{cases} \quad (2a)$$

$$\phi_2 = \begin{cases} \pi - \arctan(Z_0/X), & X > 0 \\ -\arctan(Z_0/X), & X < 0 \end{cases} . \quad (2b)$$

The simplified equation can be represented as,

$$\phi = n\pi - \arctan(Z_0/X) + \psi \quad (2c)$$

where n is an integer and Z_0 is the characteristic impedance of the transmission line. Here, ψ is the adjusting constant which is generally used for obtaining reasonable circuit parameter of a TL [16]. In this paper, ψ is not used for designing an isolation circuit.

For reference, a more rigorous equation considering the term α is also represented as

$$\phi = n\pi - \frac{\arg\left\{(\alpha^2 + X^2 - Z_0^2) + j2Z_0X\right\}}{2} + \psi. \quad (2d)$$
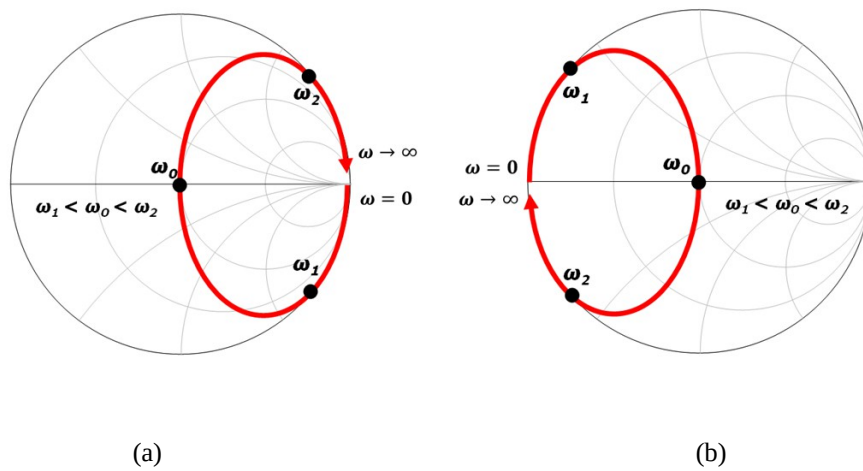

(a) (b)

Fig. 4. Locus of input impedance of a BPF shown in the Smith chart. (a) Open rejection case. (b) Short rejection case.

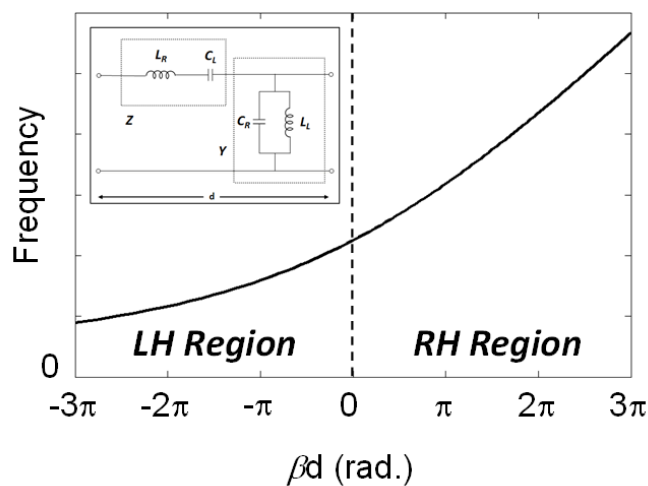

Fig. 5. Dispersion diagram of a CRLH TL (β: the propagation constant of a CRLH TL).
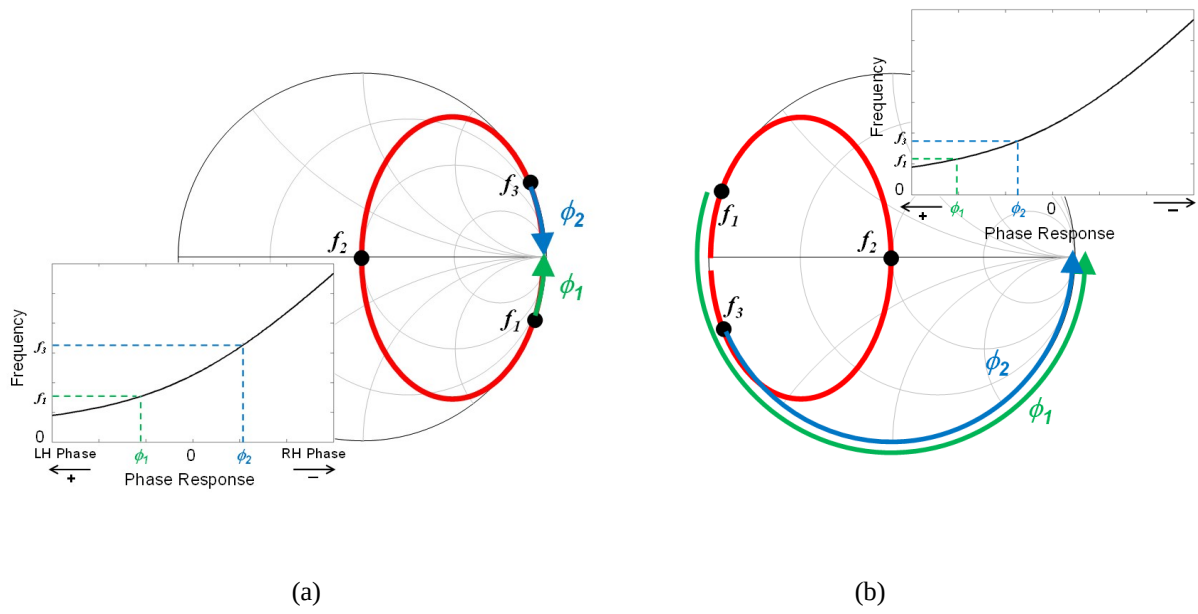
Fig. 6. Design of CRLH TL connected with f_2 filter. (a) Open rejection case. (b) Short rejection case.
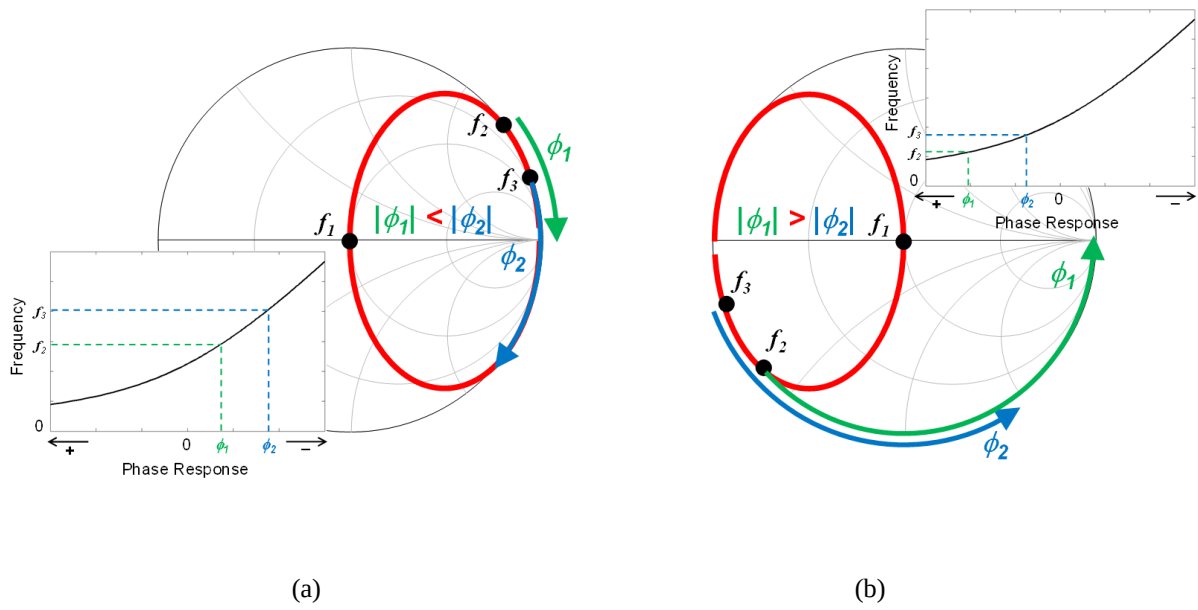

Fig. 7. Design of CRLH TL connected with f_1 filter. (a) Open rejection case. (b) Short rejection case.
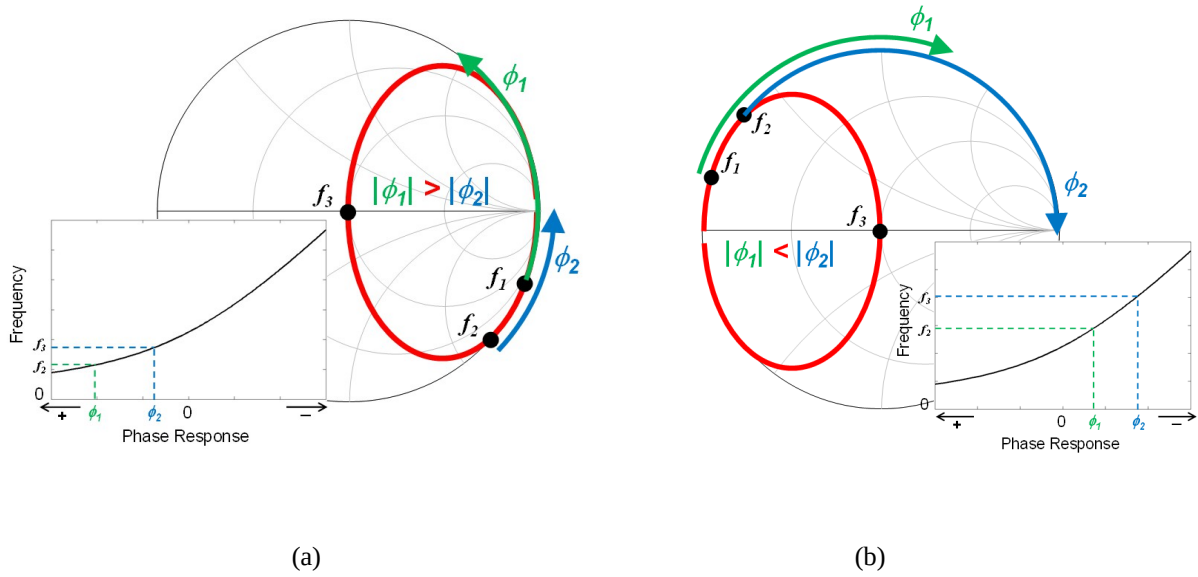
Fig. 8. Design of CRLH TL connected with f_3 filter. (a) Open rejection case. (b) Short rejection case.

C)   A Simple Contiguous Channel Implementation of the Proposed Triplexer

The proposed triplexer consists of a RH TL connected with a diplexer and a CRLH TL connected with a band-pass filter (BPF). The appropriate phase response of the RH TL is determined by investigating the input impedance of the diplexer at the center frequency of the filter used in the CRLH isolation circuit. Adding proper phase delay of the RH TL, the isolation circuit consisting of the diplexer can have open circuit input impedance which is not difficult to design with a RH TL. However, designing a CRLH TL for a contiguous channel triplexer is difficult or impractical in the circumstances that the filter connected with the CRLH TL has f_1 or f_3 center frequencies ($f_1 < f_2 < f_3$). The reason for this comes from the intrinsic characteristic of a BPF and a phase response of a CRLH TL. Fig. 4 shows the locus of input impedance of a BPF shown in the Smith chart. An input impedance of a BPF having open rejection characteristics, in which the input impedance of the filter becomes closer to infinite impedance as the frequency moves away from the pass-band, is represented in Fig. 4(a) while Fig. 4(b) shows that of a BPF having short rejection characteristic (closer to zero impedance as far away from pass-band). In both cases, impedance follows locus with clockwise rotation as frequency is increasing because a general BPF always has a positive group delay. Detailed explanation of this is provided in Appendix. Fig. 5 shows the phase response of a CRLH TL, and both left-handed (LH) and right-handed (RH) phase responses exist.

If a filter connected with a CRLH TL has f_2 center frequency, the input impedances of the filter at f_1 and f_3 are located on the Smith charts as shown in Fig. 6. With proper phase response of the CRLH TL, two impedance points can be moved to open-circuit impedance. Fig. 6(a) shows the open rejection case, and the CRLH TL can be designed by selecting LH and RH phase responses (phase advance and phase delay) at f_1 and f_3, respectively. In the short rejection case shown in Fig. 6(b), same strategy used in the open rejection case could be

difficult for design of the CRLH TL because required absolute phase responses at both f_1 and f_3 are large. Instead, only LH region of the CRLH TL can be used in this case. In the phase response of the CRLH TL shown in Fig. 6(b), both f_1 and f_3 belong to the LH region and the absolute phase response at f_1 has larger value than that at f_3. With this CRLH TL connected to the filter having the short rejection, open-circuit impedance can be realized at two target frequencies. This procedure cannot be used simply to a BPF (used on CRLH isolation circuit) having f_1 or f_3 center frequency. Fig. 7 shows input impedance of the f_1 filter represented on the Smith chart. In the open rejection case shown in Fig. 7(a), the impedance point at f_3 requires smaller phase delay (RH phase response) than that at f_2 for having open-circuit impedance. However, a phase delay at higher frequency is always larger than that at lower frequency in a CRLH TL. Hence, the CRLH TL cannot satisfy the requirement of the f_1 filter connected with the CRLH TL having open-circuit impedance at both f_2 and f_3. With similar procedure of the open rejection case, it is difficult to design a CRLH TL for the short rejection f_1 filter. In Fig. 7(b), the impedance point at f_2 needs less phase advance (LH phase response) than that at f_3. However, a CRLH TL cannot support such phase response in the LH region. In the case of the filter having f_3 center frequency, it is still difficult to design a CRLH TL satisfying the required phase response for a dual-band isolation circuit. Figure 8(a) shows the case of the open rejection f_3 filter. For open-circuit impedance at f_1 and f_2, less phase advance at f_1 and more phase advance at f_2 are necessary, however, it is difficult to satisfy such condition using a CRLH TL. Figure 8(b) shows the short rejection case, and more phase delay at f_1 and less phase delay at f_2 are necessary. The phase response of a CRLH TL does not support this.

Considering Fig. 6 to 8, it is found that using a filter having f_2 center frequency is easier for a CRLH isolation circuit of a contiguous channel triplexer. In addition, such case studies reveal that a star-junction triplexer, shown in Fig. 1(b), is not appropriate for a contiguous channel triplexer because CRLH TLs should be designed for f_1 and f_3 filters. However, the star-junction triplexer concept is valid in non-contiguous channel triplexers because interaction between channels is not strong and the adjusting constant ψ of (2c) can be used.
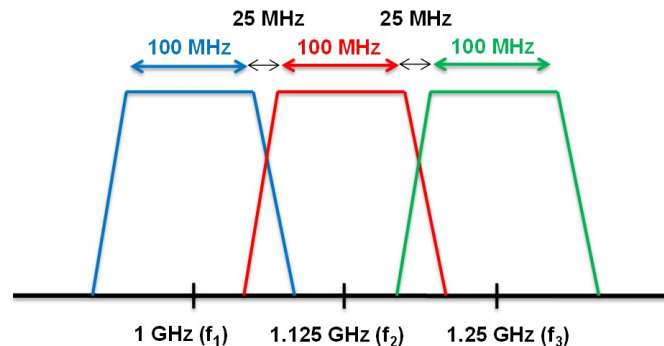

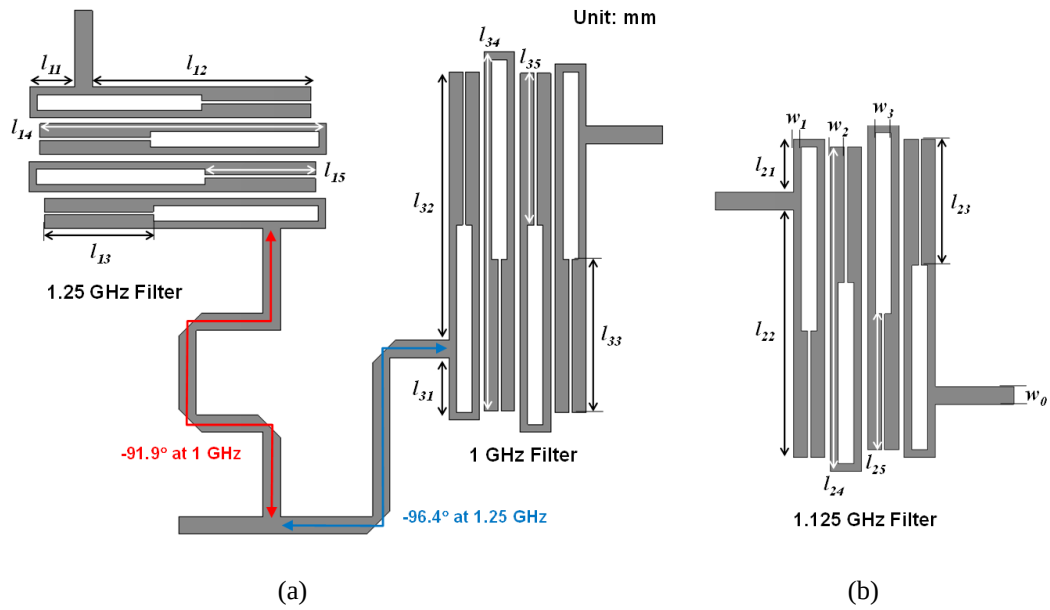Fig. 9. Ideal frequency response of proposed triplexer on output ports.

Fig. 10. The layout of filtering circuits used for proposed triplexer. (a) Diplexer. (b) 1.125 GHz filter. (Parameters: $l_{11} = 5.9$, $l_{12} = 28.55$, $l_{13} = 14.25$, $l_{14} = 37.45$, $l_{15} = 14.45$, $l_{21} = 6.8$, $l_{22} = 31.7$, $l_{23} = 16.2$, $l_{24} = 41.6$, $l_{25} = 17.4$, $l_{31} = 8.1$, $l_{32} = 35.1$, $l_{33} = 20$, $l_{34} = 46.9$, $l_{35} = 19.8$, $w_0 = 2.3$, $w_1 = 1$, $w_2 = 1.8$, $w_3 = 2$.)
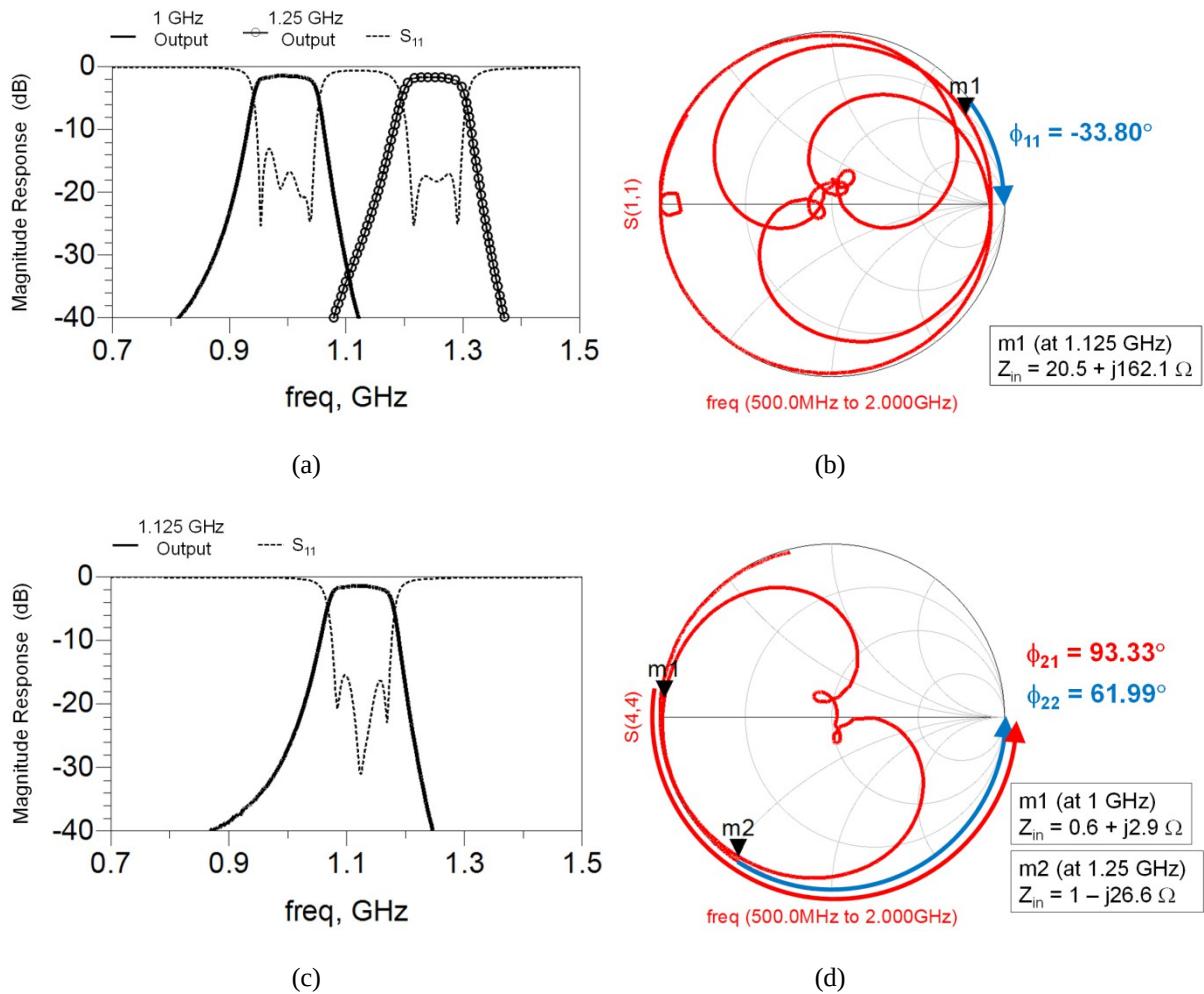

Fig. 11. Performances of the diplexer and the filter used on proposed triplexer. (a) Magnitude response of the diplexer. (b) Input impedance of the diplexer shown on the Smith chart. (c) Magnitude response of the filter. (d)

Input impedance of the filter shown on the Smith chart.

Design Process

In this section, the design process of the proposed triplexer is presented. Fig. 9 shows the frequency response of the triplexer at output ports with ideal conditions. The combination of a diplexer shown in Fig. 10(a), whose center frequencies are 1 GHz and 1.25 GHz, and a 1.125 GHz filter shown in Fig. 10(b) realizes the proposed triplexer. For compact size, hairpin-line filters are used for filtering circuits in the proposed triplexer [17]. The fractional bandwidths of the filters are around 10 %, and it could be difficult to design the proposed triplexer with use of a filter having wide bandwidth because of band limitation of an isolation circuit. For reference, the diplexer is composed with two filters and it follows the simpledesign concept of Fig. 1(a). Fig. 11(a) and (b) show the measured magnitude characteristics and input impedance of the diplexer, respectively. The measured results of the 1.125 GHz filter are shown in Fig. 11(c) and (d). The frequency configuration of the triplexer is represented in Fig. 9, and its design procedure is as follows:

1. Find an input impedance of a diplexer at the center frequency of a filter used on a CRLH isolation circuit, and check input impedances of the filter at operating frequencies of the diplexer used on the other isolation circuit. In the proposed triplexer, the input impedance of the diplexer at 1.125 GHz (marker 1 in Fig. 10(b)) and the input impedances of the 1.125 GHz filter at 1 GHz and 1.25 GHz (markers 1 and 2 on Fig. 10(d)) are necessary for our design.

2. Find the proper phase responses for each diplexer or filter using Eq. (2c) or (2d) in order to obtain open-circuit impedance at the target frequencies. In the proposed triplexer, the desired phase delay ϕ_{11} for the diplexer is -33.80°, and the required phase shifts ϕ_{21} and ϕ_{22} for the filter are 93.33° and 61.99°, respectively.

3. Calculate circuit parameters of a CRLH TL and a length of a RH TL with solved phase responses in the procedure 2 above. In the proposed triplexer, the circuit parameters of the CRLH TL are solved by submitting $(\phi_{21}, \phi_{22}) = \{1.63$ rad. $(93.33°)$, 1.08 rad. $(61.99°)\}$ and $(\omega_{21}, \omega_{22}) = (2×\pi×1$ GHz, $2×\pi×1.125$ GHz$)$ pair and N = 2 to Eq. (3)-(6) [10]. The circuit parameters of the CRLH TL are $L_R = 1.96$ nH, $C_R = 0.78$ pF, $L_L = 7.50$ nH, and $C_L = 3.00$ pF. For the diplexer, a conventional RH TL, having an electrical length of -33.80° at 1.125 GHz is necessary.

$$L_R = \frac{Z_0[\phi_{21}(\omega_{21}/\omega_{22})-\phi_{22}]}{N\omega_{22}[1-(\omega_{21}/\omega_{22})^2]} \quad (3) \qquad C_R = \frac{\phi_{21}(\omega_{21}/\omega_{22})-\phi_{22}}{N\omega_{22}Z_0[1-(\omega_{21}/\omega_{22})^2]} \quad (4)$$

$$L_L = \frac{NZ_0[1-(\omega_{21}/\omega_{22})^2]}{\omega_{21}[\phi_{21}(\omega_{21}/\omega_{22})-\phi_{22}]} \quad (5) \qquad C_L = \frac{N[1-(\omega_{21}/\omega_{22})^2]}{\omega_{21}Z_0[\phi_{21}(\omega_{21}/\omega_{22})-\phi_{22}]}. \quad (6)$$

4. Combine a diplexer with a RH TL and connect a filter with a CRLH TL. In the proposed triplexer, the CRLH TL, designed in the procedure 3, and the 1.125 GHz filter make dual-band isolation circuit, and the combination of the diplexer and the conventional RH TL makes single-band isolation circuit.

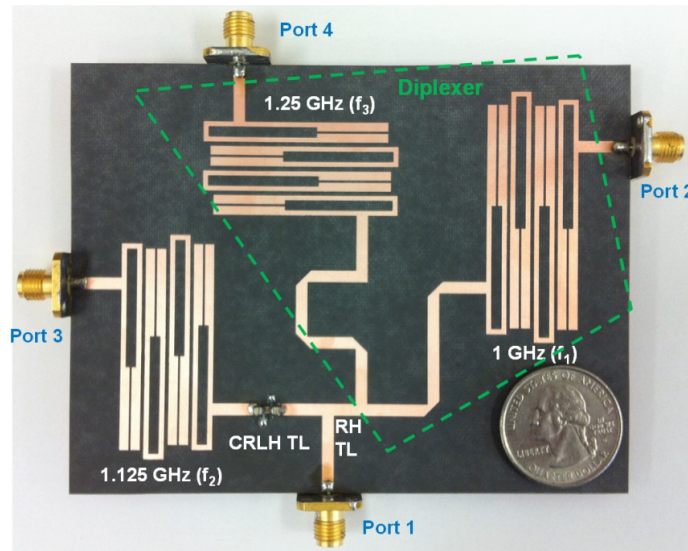5. Connect two isolation circuits with common input port.

Fig. 12. Fabricated contiguous channel triplexer based on CMTC.

TABLE I
SUMMARY OF CONTIGUOUS CHANNEL TRIPLEXER

		Circuit 1 (RH TL + Diplexer)		Circuit 2 (CRLH TL + Filter)	
Impedance of Filtering Circuits (Ω)		At 1.125 GHZ	20.5 + j162.1	At 1 GHZ	0.6 + j2.9
				At 1.25 GHZ	1 - j26.6
Required Phase Response (deg.)		ϕ_{11}	-33.80	ϕ_{21}	93.33
				ϕ_{22}	61.99
Circuit Parameters of CRLH TL (L : nH, C : pF)	L_R			1.96	
	C_R			0.78	
	L_L			7.50	
	C_L			3.00	

Ω = ohm, nH = nano henry, pF = pico farad

CONTIGUOUS TRIPLEXER

The proposed triplexer is composed of the single-band isolation circuit, a combination of the diplexer and the conventional TL, and the dual band isolation circuit, which consists of a filter

and a CRLH TL. In order to verify the design concept, the proposed triplexer is designed and fabricated. In Section III, the design process of the triplexer has been investigated, and the derived data are summarized in Table I. In the fabricated triplexer picture shown in Fig. 12, the diplexer is located on the right side of the picture and the 1.125 GHz filter is on left side. A RT/Duroid 5870 substrate (ε_r = 2.33, Height = 0.787 mm) is used for the triplexer and hairpin-line BPFs are printed on the substrate for filtering circuits [17]. The lumped elements and the microstrip lines are used to form the CRLH TL. The LH part of the CRLH TL is realized by the lumped elements, and the microstrip lines are used for the RH part. For a single band isolation circuit, the microstrip line which has 33.80° phase delay at 1.125 GHz is used.

Fig. 13 shows the simulated and measured results of the contiguous triplexer. ~~The guard bands are slightly wider than desired bandwidth, 25 MHz, which is due to the increased insertion loss near the guard bands.~~ Figure 13(a) shows the insertion losses, which are less than 1.8 dB. The measured guard bandwidth is around 25 MHz. The return losses, shown in Fig. 13(b), are larger than 10 dB, whereas Fig. 13(c) shows that the isolation is greater than 11.2 dB.

(a)

(b)

(c)
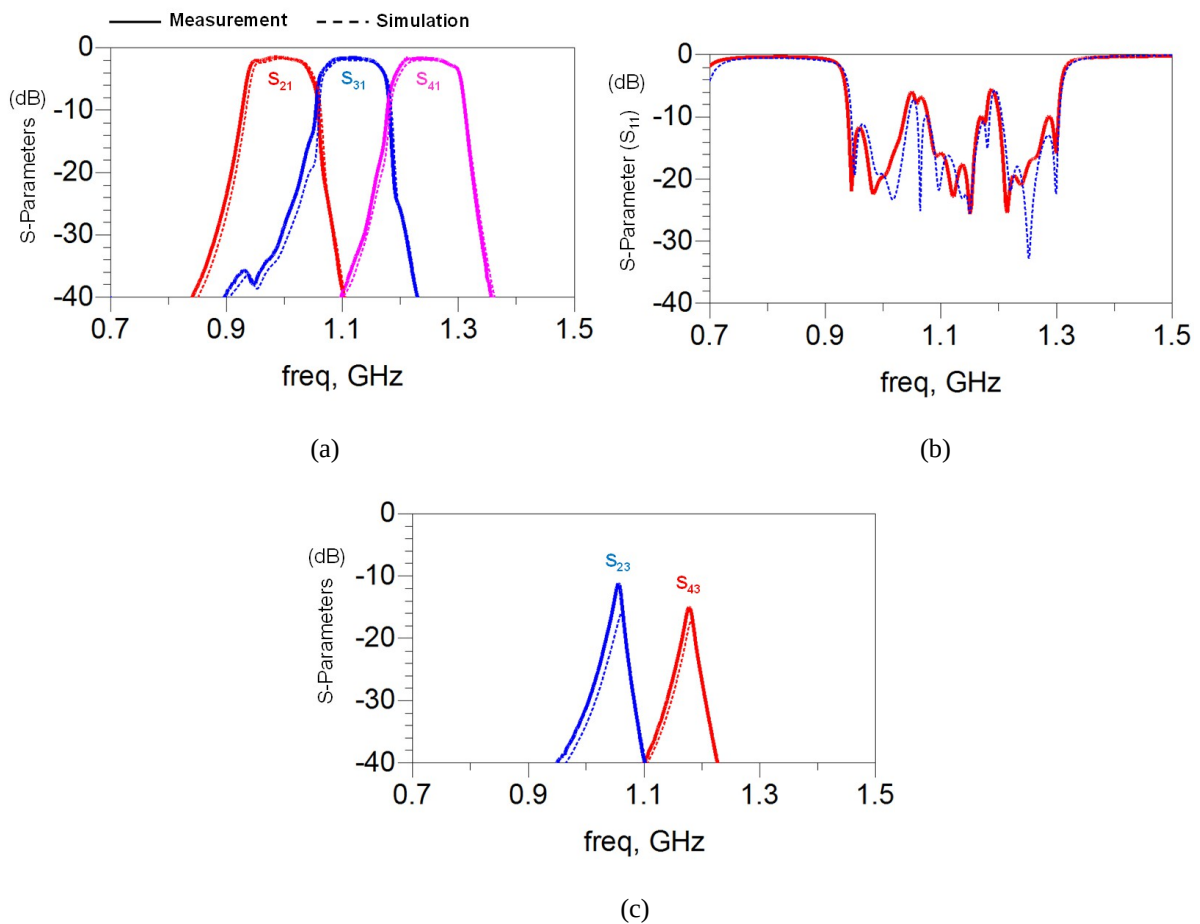
Fig. 13. Simulated and measured results of proposed triplexer. (a) Insertion loss. (b) Matching at port 1. (c) Isolation.

CONCLUSION

A contiguous channel triplexer based on CMTC has been presented. The measured results of the proposed triplexer show good agreement with the simulation results. The concept, theories, and design process have been explained to help the reader design and fabricate this type of triplexer. It is usually difficult to design a contiguous or small guard band triplexer because of the strong interaction between the channels, and a designer is required to optimize filters or use a specific filter type. However, the proposed triplexer provides straightforward and simple design method. In addition, a system designer can choose any filter or diplexer without modification. Although a star-junction triplexer based on isolation circuits also has same advantages, it is difficult or nearly impossible to design CRLH TLs for a contiguous channel triplexer. Hence, the proposed triplexer is very attractive to a system designer.

REFERENCES

[1] G. Macchiarella, "Synthesis of Star-Junction Multiplexer," *IEEE Microwave Magazine,* vol. 12, no.6, pp. 101-109, Oct. 2011.

[2] G. Macchiarella and S. Tamiazzo, "Synthesis of Star-Junction Multiplexers," *IEEE Trans. Microwave Theory Tech.,* vol. 58, no. 12, pp. 3732–3741, Dec. 2010.

[3] R. J. Cameron and M. Yu, "Design of manifold-coupled multiplexers," *IEEE Microwave Magazine,* vol. 8, no.5, pp. 46-59, Oct. 2007.

[4] E.G. Cristal and G.L. Matthaei, "A Technique for the Design of Multiplexers Having Contiguous Channels," *IEEE Trans. Microwave Teory Tech.,* vol. 10, pp. 83-93, Jan. 1964.

[5] J.D. Rhodes and R. Levy, "A generalized multiplexer theory," *IEEE Trans. Microwave Theory Tech.,* vol. 27, no. 2, pp. 99-111, Feb. 1979.

[6] K. L. Wu and W. Meng, "A direct synthesis approach for microwave filters with a complex load and its application to direct diplexer design," *IEEE Trans. Microwave Theory Tech.,* vol. 55, no. 5, pp. 1010–1017, May 2007.

[7] J.D. Rhodes and R. Levy, "Design of general manifold multiplexers," *IEEE Trans. Microwave Theory Tech.,* vol. 27, no. 2, pp. 111–123, Feb. 1979.

[8] A.E. Atia, "Computer aided design of waveguide multiplexers," *IEEE Trans. Microwave Theory Tech.,* vol. MTT-22, pp. 322-336, Mar. 1974.

[9] M.A. Ismail, D. Smith, A. Panariello, Y. Wang, and M. Yu, "EM-based design of large-scale dielectric resonator filters and multiplexers by space mapping," *IEEE Trans. Microwave Theory Tech.,* vol. 52, no. 1, pp. 386–392, Jan. 2004.

[10] H. Lee and T. Itoh, "Dual band isolation circuits based on CRLH transmission lines for triplexer application," *2011 Asia-Pacific Microwave Conference,* pp. 542-545, Dec. 2011.

[11] I. Lin, M. Vincentis, C. Caloz, and T. Itoh, "Arbitrary dual-band components using composite right/left-handed transmission lines," *IEEE Trans. Microwave Theory Tech.,* vol. 52, pp. 1142–1149, April 2004.

[12] C. Caloz and T. Itoh, *Electromagnetic Metamaterials, Transmission Line Theory and Microwave Applications,* New York: Wiley, 2005.

[13] H. Lee, J. S. Sun, and T. Itoh, "Contiguous triplexer based on combining method of two filtering circuits using CRLH and RH isolation circuits," *2013 European Microwave Conference,* Oct. 2013.

[14] H. Lee and T. Itoh, "Combining method of two filtering circuits based on isolation circuits for five-channel multiplexers," *2013 Asia-Pacific Microwave Conference,* to be published.

[15] D. M. Pozar, *Microwave Engineering,* J. Willey & Sons, 2005.

[16] H. Lee and T. Itoh, "Tri-band isolation circuits based on double-Lorentz transmission lines for quadruplexers," *2012 European Microwave Conference,* pp. 585-588, Oct. 2012.

[17] J.-S. Hong and M.J. Lancaster, *Microwave Filters For RF/Microwave Applications,* Wiley, New York, 2011.

[18] R. Schaumann and M. E. V. Valkenburg, *Design of Analog Filters,* New York, Oxford: Oxford University Press, 2001.

APPENDIX

A second-order BPF has the transfer function of reflection coefficient of following mathematical form:

$$H_{ref}(s) = \frac{A(s^2 + \omega_0^2)}{s^2 + (\omega_0/Q)s + \omega_0^2} = A\frac{(s - z_1)(s - z_2)}{(s - p_1)(s - p_2)}. \quad (7)$$

where $s = \sigma + j\omega$, which is the complex frequency, ω_0 is the center frequency of the BPF, and Q stands for the quality factor. In addition, the constant A accounts for the rejection type at DC and infinite frequency ($\omega \to \infty$). If the stop band input impedance is infinite (open), A is equal to 1, whereas if the input impedance is zero (short) then A becomes -1. The above equation can be further expressed with the factored form in terms of poles (p_i) and zeros (z_i).

It is found useful that the frequency response of reflection coefficient S_{11} can be visualized through the use of pole-zero plots. As an illustrative example shown in Fig. 14, four different frequencies from low to high ($\omega = 0$, $\omega = \omega_1$, $\omega = \omega_0$, and $\omega = \omega_2$) are picked in order to examine the frequency response of the transfer function.
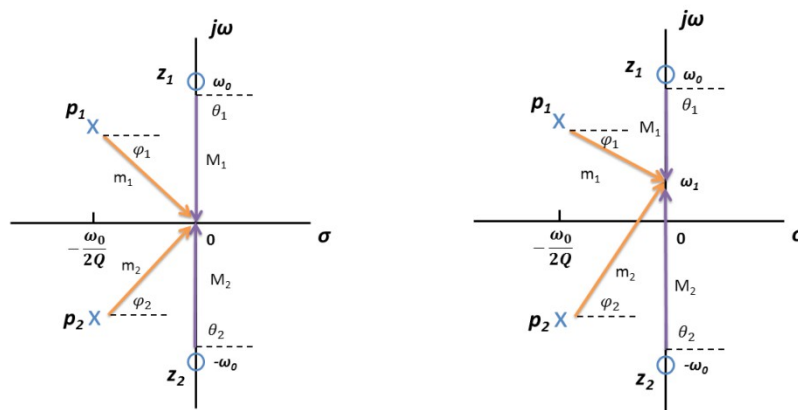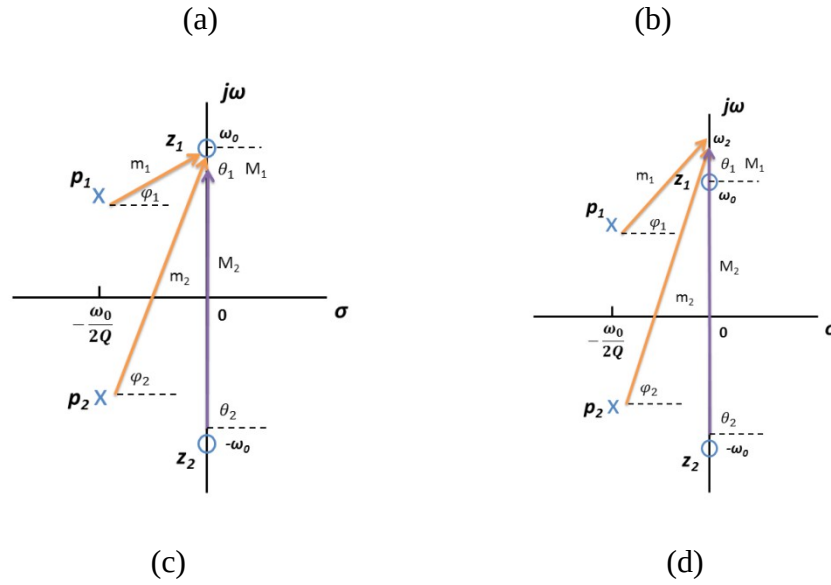
Fig. 14. Pole-zero plots of the transfer function of reflection coefficient at (a) $\omega = 0$, (b) $\omega = \omega_1$, (c) $\omega = \omega_0$, and (d) $\omega = \omega_2$
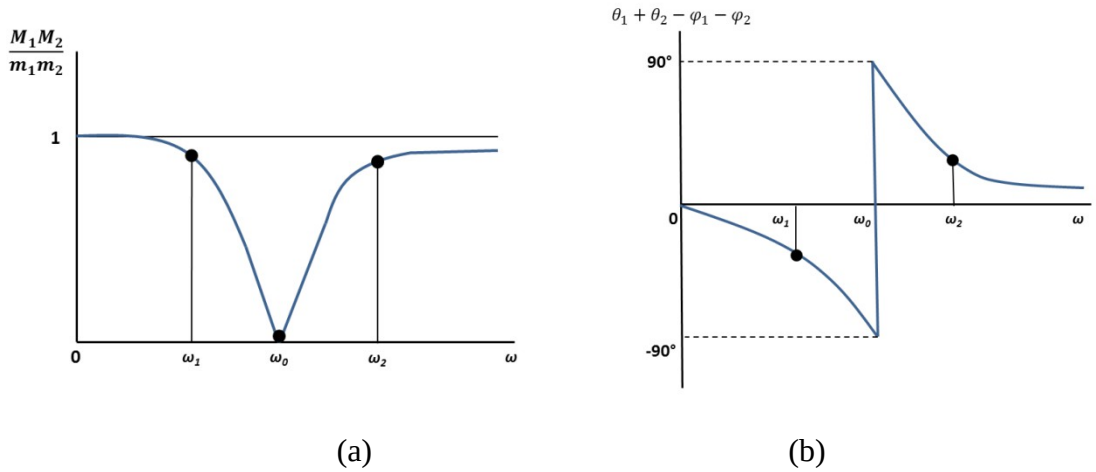

Fig. 15. (a) Amplitude and (b) phase response of the reflection coefficient of a BPF

We can then construct frequency responses of the amplitude and phase from Fig. 14. By denoting the magnitude and phase of the pole vectors to be m_i, φ_i, and those of the zero vectors to be M_i, θ_i, where $i = 1, 2$, we can plot the amplitude response of the transfer function ($M_1 M_2 / m_1 m_2$) and its phase response ($\theta_1 + \theta_2 - \varphi_1 - \varphi_2$) as depicted in Fig. 15 [18]. One can observe that the reflection zero occurs at ω_0, and at this frequency the phase experiences an abrupt change from -90 degrees to +90 degrees. Overall, the phase is decreasing with respect to the frequency, which implies the transfer function of reflection coefficient has a positive group delay. As a result, the overall phase of the transfer function will be decreasing. Furthermore, if we plot the response on Smith charts, such characteristics will result in a clockwise rotation of S_{11} with frequency increasing. Fig. 4 plots the corresponding responses of S_{11} or input impedance of the filter when the rejection is open ($A = 1$) and short ($A = -1$), and they both rotate clockwise on the Smith charts.

Although the case discussed here is for a second order BPF, any high order BPFs' transfer functions can be decomposed to a multiplication of second order BPFs. Therefore, the same analysis can be used and will still result in the same conclusion for the sense of phase rotation.

Bibliographies
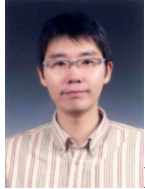
Hanseung Lee received the B.S. degree from the Korea University, Seoul, Republic of Korea, in 2006, and the M.S. degree from the Seoul National University, in 2008, both in electrical engineering and he is currently working toward the Ph.D. degree in electrical engineering from the University of California at Los Angeles (UCLA).

Since September 2010, he has been a Graduate Student Researcher at the Microwave Electronics Laboratory, UCLA. His research interests include design of a passive circuit and an antenna for RF/microwave, and applications of metamaterials.

Mr. Lee is the recipient of Asia–Pacific Microwave Conference (APMC) 2011 Prize.

Chung-Tse Michael Wu received his B.S. degree from National Taiwan University (NTU) and M.S. degree from University of California at Los Angeles (UCLA) in 2006 and 2009, respectively, both in Electrical Engineering. He is currently working toward the Ph.D. degree in the Department of Electrical Engineering, University of California at Los Angeles (UCLA).

Since September 2008, he has been a Graduate Student Researcher at the microwave electronics laboratory in UCLA. In 2009, He worked as a summer intern in Bell Laboratories, Alcatel-Lucent, Murray Hill, NJ. He is the recipient of Asia Pacific Microwave Conference (APMC) 2011 student prize. His research interests include active antennas, microwave systems and metamaterials.

Tatsuo Itoh received the Ph.D. Degree in Electrical Engineering from the University of Illinois, Urbana in 1969. After working for University of Illinois, SRI and University of Kentucky, he joined the faculty at The University of Texas at Austin in 1978, where he became a Professor of Electrical Engineering in 1981. In January 1991, he joined the University of California, Los Angeles as Professor of Electrical Engineering and holder of the TRW Endowed Chair in Microwave and Millimeter Wave Electronics (currently Northrop Grumman Endowed Chair). He received a number of awards including IEEE Third Millennium Medal in 2000, and IEEE MTT Distinguished Educator Award in 2000. He was elected to a member of National Academy of Engineering in 2003. In 2011, he received Microwave Career Award from IEEE MTT Society.

He has 420 journal publications, 820 refereed conference presentations and has written 48 books/book chapters in the area of microwaves, millimeter-waves, antennas and numerical electromagnetics. He generated 75 Ph.D. students.

List of figures and tables

Fig. 9. Ideal frequency response of proposed triplexer on output ports.

Fig. 10. The layout of filtering circuits used for proposed triplexer. (a) Diplexer. (b) 1.125 GHz filter. (Parameters: $l_{11} = 5.9$, $l_{12} = 28.55$, $l_{13} = 14.25$, $l_{14} = 37.45$, $l_{15} = 14.45$, $l_{21} = 6.8$, $l_{22} = 31.7$, $l_{23} = 16.2$, $l_{24} = 41.6$, $l_{25} = 17.4$, $l_{31} = 8.1$, $l_{32} = 35.1$, $l_{33} = 20$, $l_{34} = 46.9$, $l_{35} = 19.8$, $w_0 = 2.3$, $w_1 = 1$, $w_2 = 1.8$, $w_3 = 2$.)

Fig. 11. Performances of the diplexer and the filter used on proposed triplexer. (a) Magnitude response of the diplexer. (b) Input impedance of the diplexer shown on the Smith chart. (c) Magnitude response of the filter. (d) Input impedance of the filter shown on the Smith chart.

Fig. 12. Fabricated contiguous channel triplexer based on CMTC.

Fig. 13. Simulated and measured results of proposed triplexer. (a) Insertion loss. (b) Matching at port 1. (c) Isolation.

Fig. 14. Pole-zero plots of the transfer function of reflection coefficient at (a) $\omega = 0$, (b) $\omega = \omega_1$, (c) $\omega = \omega_0$, and (d) $\omega = \omega_2$.

Fig. 15. (a) Amplitude and (b) phase response of the reflection coefficient of a BPF.

Table 1. Summary of contiguous channel triplexer.